

The Momentum Flux Balance at the Sea Surface

Donald Resio and Charles Long
Coastal and Hydraulics Laboratory
Army Engineer Research and Development Center
3909 Halls Ferry Road, Vicksburg, MS

1. Introduction

Today, second- and third-generation wave models are used for many applications around the world. From the design of coastal structures to proper regional sediment management and from estimates of mixing in the upper ocean to the efficient the routing of ships across oceans, the accuracy of these models has critical importance. However, following the development of the WAM model in the mid to late 1980's, there has been little effort focused directly on wave model development. Instead, most research in this area has involved re-calibrating various source terms to obtain better fits to observations (satellite and *in situ*). Two likely reasons for the lack of focus in this area are 1) the general acceptance outside of the wave community that the WAM model physics provided a good "detailed-balance" description of the wave generation process and 2) wave researchers cannot agree on necessary modifications to the WAM physics. The purpose of this paper is to revisit the general framework of the physics of wave generation and attempt to formulate a concept for wave generation that seems to "fit" some important constraints implicit in observations over a wide range of generation scales (time and space). Toward this end, data from three very different sites will be used:

1. Lake George – a small, shallow site located in Southeast Australia (Figure 1);
2. FRF Gage #630 – a coastal site located in the Atlantic Ocean in a depth of about 18 meters of water approximately 5 km off the coast of Duck, North Carolina (Figure 2); and
3. NDBC Buoy 46035 – an open-ocean site located in deep-water in the Bering Sea (Figure 3).

These sites cover a wide range of practical wave generation scales, from shallow to deep and from very small fetch to extremely large fetch.

2. Theoretical Framework

Ever since the mid 1970's, most simulations of the evolution of wave spectra under the action of the wind have included the effects of wave-wave interactions. Unfortunately, this nonlinearity effectively couples the entire wave spectrum into a single dynamic system, making it difficult to assess the precise roles of different forcing

mechanisms. In an attempt to avoid this problem, we postulate a theoretical framework for wind-wave spectra during active wave generation as shown in Figure 4. In this Figure, four spectral regions are defined, based roughly on the hypothesized controlling forcing mechanisms for each region.

Region 1, the spectral peak region, is bounded at its upper limit by frequency f_0 , which is a frequency at which there is no net nonlinear flux of energy and extends to zero at its lower limit. Since there is no net flux of energy into or out of Region 1 due to wave-wave interactions, the net gain or loss of energy in this region depends only on external sources (wind input and wave breaking). The role of wave-wave interactions region will likely relate to down-shifting of the spectral peak, due to the strong asymmetry of this source term within this region.

Region 2, the transition region from Region 1 to the equilibrium range, is bounded by f_0 at its lower limit and by f_{eq} (the low-frequency limit of the equilibrium range) at its upper boundary. This region represents an area in which nonlinear energy fluxes become less and less influenced by the proximity to the spectral peak (and low-frequency cut-off) as f_{eq} is approached. Since there is zero net energy flux across f_0 , we will hypothesize here that the primary mechanisms controlling the shape of this region are net wind input and wave-wave interactions. Under the assumption that wave breaking is very small in this region, a positive flux of energy (i.e. a flux directed toward high frequency) must exist at f_{eq} , in order to compensate for the energy gain in this region.

Region 3, the equilibrium range, has been the subject of many studies (Zakharov and Fileneko, 1966; Kitaigorodskii, 1983; Resio, 1987; Resio *et al*, 2001). It is assumed here that this region extends from f_{eq} at its lower limit to some high frequency at which dissipation begins to play a major role in the spectral energy balance. In the initial derivation by Zakharov and Fileneko (1966), it was assumed that an ω^{-4} (where ω is radial frequency) slope would exist in this region (i.e. $E(\omega) \sim \omega^{-4}$, where $E(\omega)$ is energy density) in the absence of any external sources and sinks. However, since we know that wind input exists at the spectral peak and at higher frequencies, it is extremely unlikely that wind input is identically zero across the entire equilibrium range. Consequently, it would appear that the requirement of no input should be relaxed to a sufficiently small input such that the equilibrium slope is not moved far from the ω^{-4} slope observed in most deep-water data sets. Recently, Resio *et al* (2001) showed that a more general form for the equilibrium range could be written in term of a wavenumber spectrum,

$$F(k) = \frac{\alpha_4}{2} u_s g^{-1/2} k^{-5/2} \quad (1)$$

where $F(k)$ is the energy density in wavenumber space, α_4 is a universal constant, u_s is a scaling velocity , g is gravity, and k is wavenumber.

We assume that all three traditional deep-water source terms, wind input (S_{in}), nonlinear wave-wave interactions (S_{nl}), and wave breaking (S_{ds}), occur in all regions of

the spectrum to some degree. For a stable equilibrium to exist, the sum of all three sources must equal zero. In the equilibrium range, if the sum of the wind and wave breaking source terms are not zero, S_{nl} , which is equal to the divergence in the nonlinear energy fluxes, must be non-zero to maintain a net zero balance. In other words, we would have

$$\frac{\partial \Gamma_E}{\partial \mathbf{w}} = S_{in} + S_{ds} \quad (2)$$

where Γ_E is the flux of energy through the spectrum. If wind input and wave breaking exactly cancel each other in this range, equation 2 would still hold. It would only mean that the divergence would be identically zero over this range and the fluxes should be exactly constant.

Nonlinear energy fluxes transfer energy from low to high frequencies and from high to low frequencies simultaneously. In some previous papers, the term flux has been used to describe the positive-directed fluxes (fluxes from low to high frequency), while the negative-directed fluxes (fluxes from high to low frequency) are termed inverse fluxes; however, this terminology will not be adopted here. We shall take the meaning of Γ_E to be the net difference of the fluxes in both directions, i.e.

$$\Gamma_E = \Gamma_E^+ + \Gamma_E^- \quad (3)$$

where the superscripts “+” and “-” denote fluxes toward higher and lower frequencies, respectively. According to essentially all recent theoretical treatments of S_{nl} , nonlinear fluxes within the equilibrium range tend to force the spectrum toward an ω^{-4} spectral form in the absence of other significant source terms. However, as will be shown here, even for typical wind inputs, the deviation from an ω^{-4} spectral form may be quite small. Within the equilibrium range, the flux of energy from lower to higher frequencies is given by (Resio *et al.*, 2001) in a form equivalent to

$$\Gamma_E^+ = C_{nl} \sqrt{g} \mathbf{b}^3 \quad (4)$$

where C_{nl} is a dimensionless coefficient depending weakly on angular spreading and proximity to the spectral peak and β is a wave steepness parameter equivalent to $\alpha_4 u / (2g^{1/2})$ in equation 2. To a first approximation, the divergence of the flux can be written as

$$\frac{\partial \Gamma_E^+}{\partial \mathbf{w}} \sim \frac{\partial \mathbf{x}^3}{\partial \mathbf{w}} \quad (5)$$

where ξ is a compensated spectral density of the form

$$\mathbf{x} = \frac{2F(k) g^{1/2} k^{5/2}}{\mathbf{a}_4 u} \quad (6)$$

From these arguments it can be seen that a 20% increase in spectral densities in the equilibrium range would result in over a 70% increase in the energy flux rates due to nonlinear interactions. Thus, the nonlinear interactions should force a very strong tendency toward the ω^{-4} spectral form even if wind input is occurring in this region of the spectrum.

Region 4, the dissipative range, is the portion of the spectrum in which energy, fluxed toward high frequencies via nonlinear interactions, is lost due to either turbulence (breaking) or viscous effects. The low-frequency limit to this range should be coincident with the point where the equilibrium range slope shifts to a steeper slope (ω^{-n} where $n > 4$). This may occur over a range of frequencies and different researchers have postulated different points at which this is expected to occur. For the purpose of this paper, we will just assume that a high-frequency energy sink exists, one that is capable of removing all energy fluxed into this region of the spectrum. Since this spectral region is located at relatively high frequency, the exact shape of the spectrum in this region does not affect most practical applications.

3. Data

Data selected for analysis here include one deep ocean buoy maintained by the National Data Buoy Center (NDBC, <http://www.ndbc.noaa.gov>), one shallow ocean sensor maintained by the U.S. Army Engineer Research and Development Center's Field Research Facility (FRF, <http://www.fr.usace.army.mil>), and one site on the east side of Lake George, Australia. Anemometers were located directly above wave sensors at all sites except for FRF #630, where winds were measured at the landward end of the FRF pier.

Four dimensionless parameters can be considered relative to site selection: relative depth of the waves in the equilibrium range, $k_{eq}h$, relative wave height H_{mo}/h , wave steepness $H_{mo}k_p$, and inverse wave age u_a/c_p (often characterized as u_{10}/c_p). The first of these has an approximate theoretical lower limit $k_{eq}h \approx 0.7$ below which the wavenumber dependence of the equilibrium range may change form, due to depth-related changes in the behavior of coupling coefficient (Resio 1987). Zakharov (1999) has shown that for $k_{eq}h < 0.3$, the spectrum should asymptotically tend toward a $k^{-4/3}$ form. The subscript "eq" has been added to his original "kh" parameter to reflect the fact that his theoretical argument is valid only within the equilibrium range and not in the spectral peak region. With parameters defined in Sections 3.2 and 3.3, data from the above sites have relative depths in the range $0.7 < k_{eq}h$, which pushes the lower limit somewhat. The data extends into very deep water at most deep-ocean sites.

4. Analysis

Figure 5 shows a plot of the band-averaged value for ξ as a function of f/f_p , for all three data sets described later in this paper. In this Figure, the subscript “p” denotes a value at the spectral peak. Also shown in this Figure are the curves for k^{-3} (ω^{-5} equivalent in deep water) and k^{-2} (ω^{-3} equivalent in deep water) spectra, which clearly do not fit the data very well. Even though some random deviations and some possibly periodic variations in the value of ξ are seen, the general tendency is for ξ to remain approximately constant in all of the data sets.

Since we are interested here in an integral balance of energy, rather than a detailed frequency-direction balance, we shall not attempt to build upon different source term forms; rather, we shall examine six types of wind-input scaling. These can be written in the form:

$$\int_{f_0}^{f_{eq}} S_{in}(f)df \sim u_a^3 \quad (7)$$

and

$$\int_{f_0}^{f_{eq}} S_{in}(f)df \sim u_a^2 c_p \quad (8)$$

where c_p is the phase speed of waves at the spectral peak, u_a is a scaling parameter with units of velocity, taken here to be 1) the wind speed at a reference level of 10 meters (u_{10}); 2) the friction velocity ($u_* = \tau^{1/2}/\rho_a$, where τ is the wind stress and ρ_a is air density); and 3) the wind speed at a fractional height of the wavelength of the spectral peak (u_λ as defined in Resio, *et al.*, 1999). Thus, the six scaling combinations investigated here consist of three different scaling parameters for wind speed inserted into the two different scaling forms shown in equations 7 and 8.

4. Results

Figures 6a-6c show a plot of β versus $\frac{u_a}{\sqrt{g}}$, where u_a , in turn, represents the three scaling options based on wind speed parameters only. Clearly, this scaling option does not provide a unified scaling form for the different data sets. Instead, the slope of the small-basin data (Lake George) is considerably shallower than the slope of the open ocean data sets (FRF #630 and NDBC 46035). Figures 7a-7c show a plot of β versus $\frac{u_a}{\sqrt{g}}$, where u_a , in turn, represents the three scaling options based on wind speed and phase velocity parameters in the manner described above. This scaling velocity provides a basis for the data in the slopes of each data set are all consistent. Thus, this scaling, rather than a scaling based on wind speed alone, provides a better, scale-independent representation for energy densities in the equilibrium range.

Of the three different velocity scales examined, the velocity referenced at a level of 0.065 times the peak wavelength above the mean surface consistently provided the scaling relationship with the lowest scatter around the regression line. In fact as shown in Resio *et al* (2002), this scatter is reduced by a factor of three to four in high-quality, small-basin data sets.

4. Discussion

As shown in Resio *et al* (2002), the findings here are consistent with a constant flux of momentum from the atmosphere into the wave field, which agrees with the work of Hasselmann *et al* (1973) and Resio and Perrie (1989). In fact, in the work by Resio and Perrie (1989) was the initial basis for attempting the $u_a^2 c_p$ form as the scaling parameter for β , after we had found that none of the forms based on wind speed alone gave a very good result.

The best-fit relationship for the entire data set was clearly achieved with the $u_r^2 c_p$ scaling parameter. If we return to the work of Resio and Perrie (1989), we see that they included an analysis of laboratory data in their scaling analysis and showed that a $u_{10}^2 c_p$ form provided a better fit to a wide range of data than did forms based on wind speed alone; however, they did not have the extensive data shown here supporting that conclusion in their paper. If we return to the data sets shown in their paper we see that the use of u_r improves the consistency of the β - u_a relationship for lab data included.

These findings could potentially have significance to at least three several practical applications. First, the interpretation of scatterometer data is roughly based on a linear relationship between wind speed and measured return from wave fields. Since the calibration of this relationship is based primarily on open-ocean data, it is possible that the actual relationship is more of the form shown here. Second, wave models that depend on detailed-balance arguments, typically have been calibrated to reflect either an ω^{-5} spectral form or a linear dependence of the energy levels in the equilibrium range on wind speed. It is unlikely that either of these detailed-balance forms can work well over a wide range of dynamic scales. And third, arguments of wave induced drag coefficients, which are strongly dependent on wave age, are not supported by our findings.

Another point worth discussing in this paper is the fact that considerable evidence supporting the $k^{-5/2}$ equilibrium range, even into kh values as low as 0.6, is beginning to accumulate. This is consistent with the expected behavior of spectral energy densities in the equilibrium range, based on nonlinear energy fluxes; but it is difficult to see how any wave breaking mechanism, which may be coerced to depend on f^4 in deep water, can be made to scale appropriately to reproduce this result. This appears to support arguments that the primary energy losses within a wave spectrum are located in at high frequencies and not in Regions I-III of the spectrum. It is also consistent with physical arguments based on the depth of the “turbulence” (white-capping) region at the water surface during

wave generation, since $\frac{\delta z}{L_p} \ll 1$, where δz is the depth of the white-capping region and L_p is the wavelength of the spectral peak.

5. Conclusions

The two primary conclusions based on the analyses and data sets presented here are as follows:

1. Energy densities in the equilibrium range depend on a combination of wind speed and spectral peak phase speeds, consistent with the concept that a constant proportion of the momentum transfer from the atmosphere enters the wave field.
2. Wind inputs into waves appear to scale better with wind speeds measured at a peak wavelength scaled level above the surface than with either friction velocity or winds at a fixed height.

REFERENCES

- Hasselmann, D.E., Dunckel, M., Ewing, J.A.: 1973. "Directional Wave Spectra Observed during JONSWAP 1973." *Journal of Physical Oceanography*, 10, 1264 – 1280.
- Kitaigorodskii, S.A. 1983 "On the Theory of the Equilibrium Range in the Spectrum of Wind-Generated Gravity Waves." *Journal of Physical Oceanography*, 13, 816 – 826.
- Resio, D.T., Long, C.E., and C.L. Vincent: 2002. "A Universal Equilibrium Range Constant Wind-Generated Waves, submitted for publication
- Resio, Donald T. 1987: "Shallow Water Waves. I –Theory." *J. Waterway, Port, Coastal and Ocean Engr.* 113, 264-281.
- Resio, Donald and Perrie, W: 1989. "Implications of an f-4 Equilibrium Range for Wind-Generated Waves." *Journal of Physical Oceanography*, 19, 193-204.
- Resio, Donald T., Pihl, J.H., Tracy, B.A., Vincent, C.L.: 2001. "Nonlinear Energy Fluxes and the finite Depth Equilibrium Range in Wave Spectra," *Journal of Geophysical Research*. 106, C4, 6985-7000.
- Resio, Donald T., Swail, V.R., Jensen, R.E., and Cardone, V.J: 1999 "Wind Speed Scaling in Fully Developed Seas," *Journal of Physical Oceanography*. 29, 1801-1811.
- Zakharov, Vladimir 1999: "Statistical Theory of Gravity and Capillary Waves on the Surface of A Finite-Depth Fluid," *European Journal of Mechanics*, 18, 3, May –June.

Zakharov, V.E. and Filonenko: 1966. "The Energy Spectrum for Stochastic Oscillation of a Fluid's Surface," *Doklady, Akad.Nauk*, 170, 1992-1995.

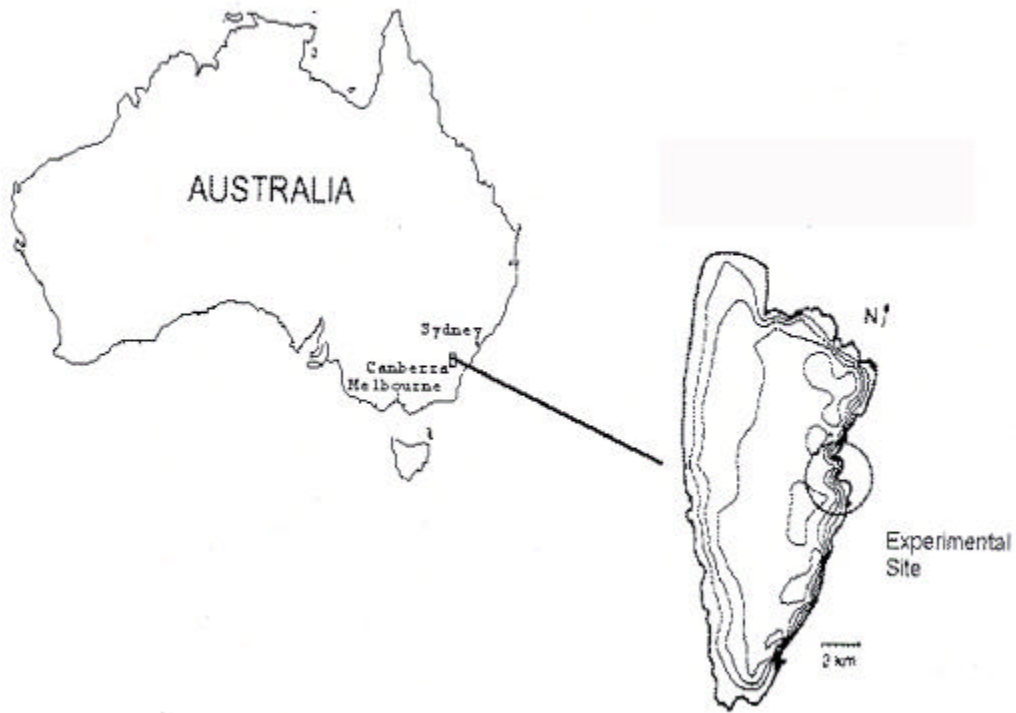


Figure 1. Location of Lake George data site.

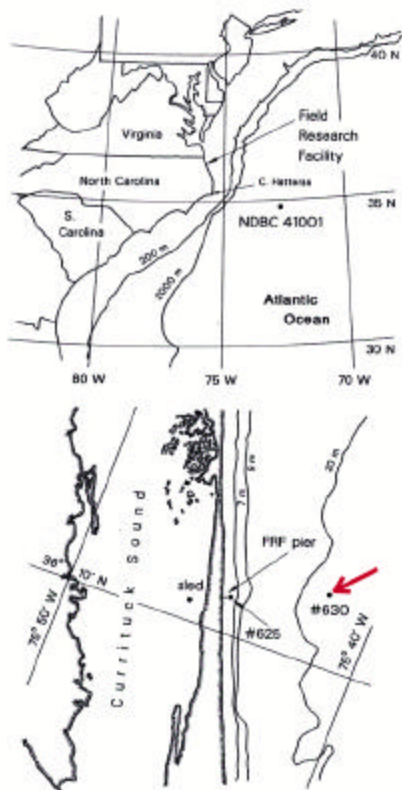


Figure 2. Location of FRF #630 site.

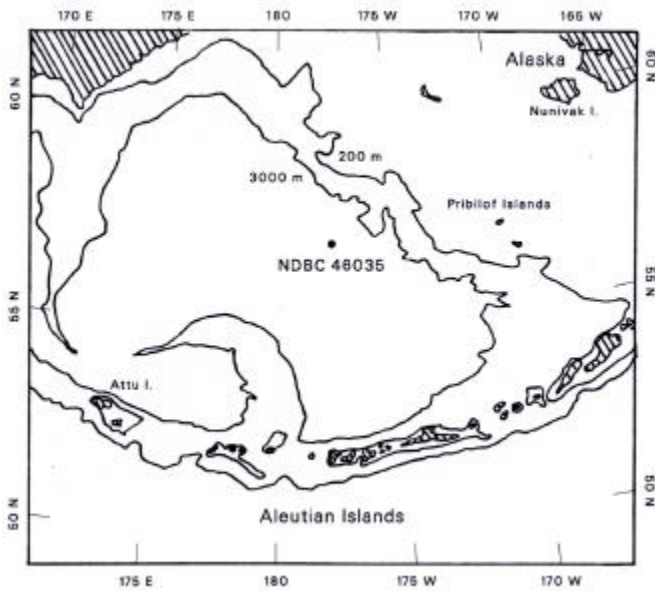


Figure 3. Location of NDBC #46035 site.

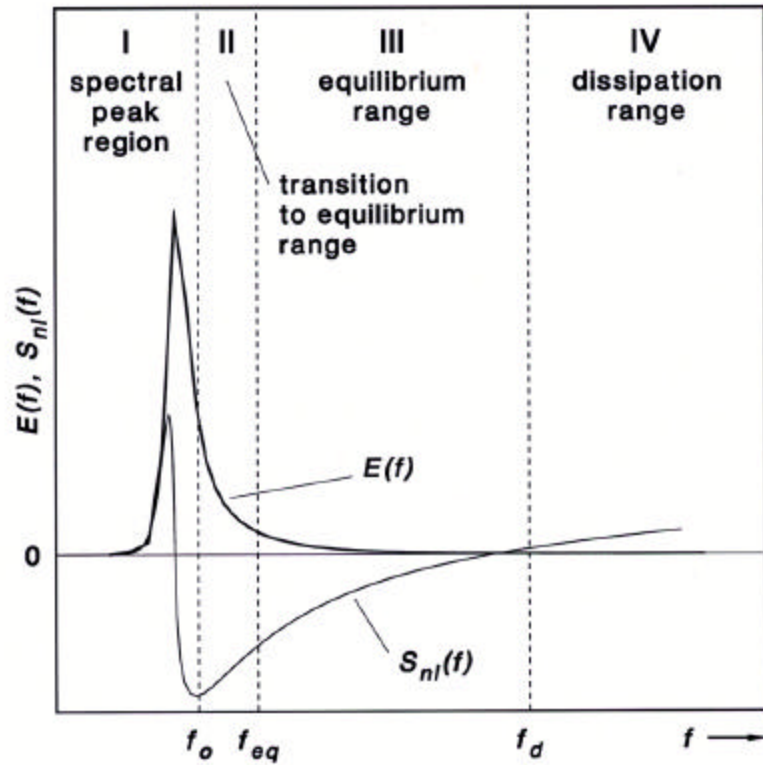


Figure 4. Schematic of diagram for spectral energy-flux regions.

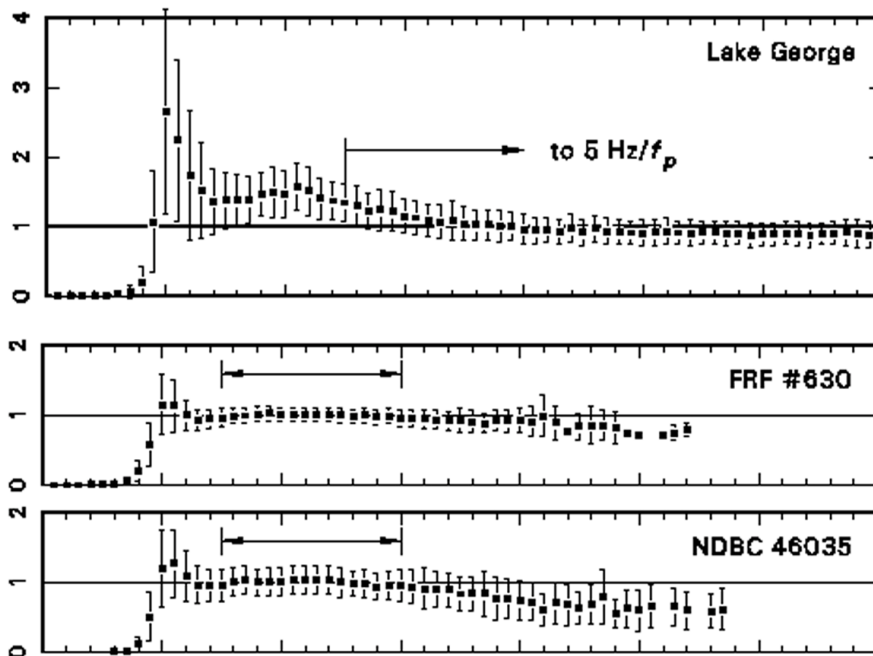
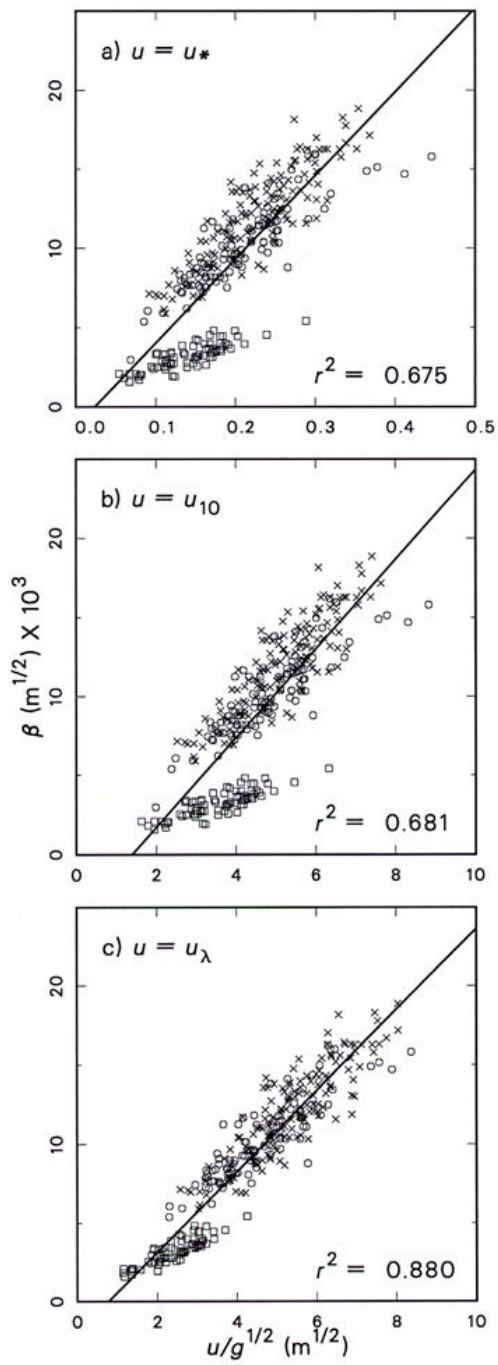
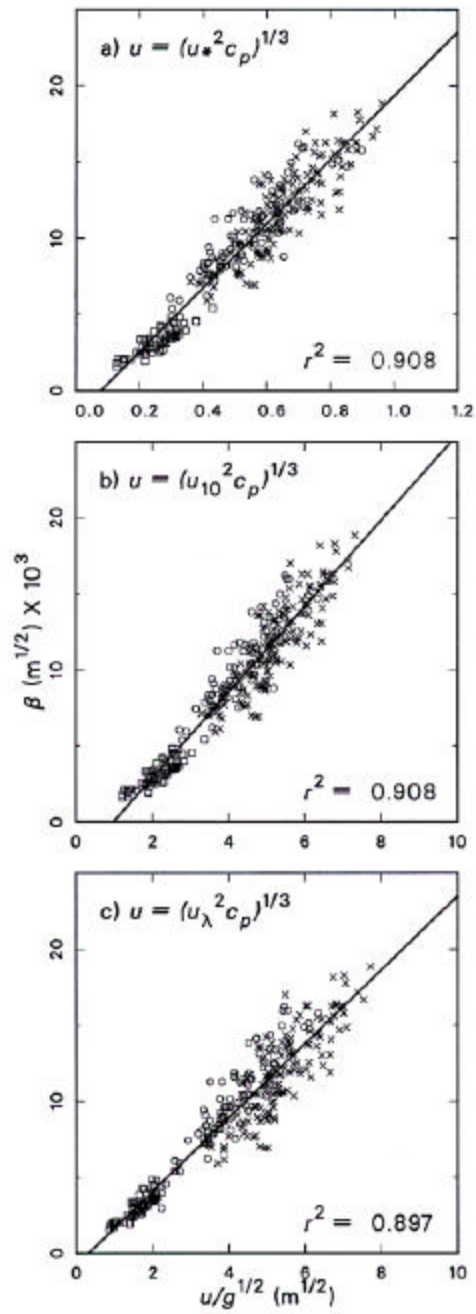


Figure 5. Behavior of spectral density at data site.



Figures 6a – c.



Figures 7a – c.